Energy 36 (2011) 5968–5974

Contents lists available at SciVerse ScienceDirect

Energy

journal homepage: www.elsevier.com/locate/energy

A novel method for the determination of dynamic resistance for photovoltaic modules

Jen-Cheng Wang[1], Jyh-Cherng Shieh[1], Yu-Li Su, Kun-Chang Kuo, Yen-Wei Chang, Yu-Ting Liang, Jui-Jen Chou, Kuo-Chi Liao, Joe-Air Jiang*

Department of Bio-Industrial Mechatronics Engineering, National Taiwan University, 1, Sec.4, Roosevelt Road, Taipei 10617, Taiwan

ARTICLE INFO

Article history:
Received 16 March 2011
Received in revised form
24 July 2011
Accepted 12 August 2011
Available online 7 September 2011

Keywords:
Dynamic resistance
Photovoltaic (PV) modules
p-n junction semiconductor
Direct resistance-estimation method

ABSTRACT

Obtaining the maximum power output in real time is indispensable to the operation of grid connected photovoltaic (PV) power systems under given atmospheric conditions. Focusing on the resistance effect of the solar cells, we propose a new and simple method to directly determine the dynamic resistance of the PV modules from an irradiated current–voltage characteristic curve. In our method, we develop the ability to determine the dynamic resistance with a combination of finite series- and shunt-connected resistance. A series of experiments, including numerical simulations and field data tests, are conducted to examine the dynamic behavior of the PV modules during power tracking. Experimental results show that the proposed direct resistance-estimation method allows the PV modules to achieve their maximum power and impedance matching under various operation conditions.

1. Introduction

Many researches on photovoltaic (PV) energy for various applications have been conducted in recent years, as a consequence of the unique properties of PV arrays [1–4]. There have also been extensive studies on improving the characteristics of renewable energy for such PV arrays, which are potentially very important for the reduction of certain carbon dioxide emissions [5–7]. The need for energy-efficient electrical power sources in remote locations is a driving force for the investigation of integrated energy systems. In particular, advancement in wind and PV generation technologies has been applied to wind-alone [8], PV-alone [9,10], and hybrid wind/PV configurations [11–13]. PV arrays have also become a reliable energy source that it is hoped can efficiently mitigate some of the worst effects of global warming [14–16]. Studies related to renewable energy sources, including PV arrays, are especially important for many developing countries around the world.

The PV modules exhibit an extremely nonlinear current–voltage (I–V) characteristic that varies continuously with module temperature and solar irradiation. The main electrical parameters of the solar cell — such as the short-circuit current I_{sc}, the open-circuit voltage V_{oc}, the maximum power P_{mp}, the fill factor FF, and the maximum conversion efficiency η_m — are functions of the resistance of solar cells, i.e., the series resistance R_s and the shunt resistance R_{sh} [17]. This is what causes low energy-conversion efficiency in the PV modules. Hence, it is worth paying more attention to how to efficiently control the operation of PV modules at maximum power output to the extent possible. A series resistance can be caused either by excessive contact resistance or by the resistance of the neutral regions. The series resistance R_s accounts for all voltages that drop across the transport resistances of the solar cell. Usually, R_s connects to a load or an inverter. The series resistance (R_s) can be determined by different methods under various illumination conditions, such as in the dark, constant illumination, and varying illumination, yielding different results [18]. In the standardized measurement method for solar cells, R_s is normally determined by two different illumination levels, the so-called two-curve method [19]. On the other hand, the shunt resistance (R_{sh}) usually results from any channel that bypasses the p-n junction. This bypass can be brought about by damaged regions in the p-n junction or surface imperfections. Shunt resistance R_{sh} occurs in the shunt paths with the diodes of the modeled solar cells. Shunt paths can occur across the surface of real solar cells, at pin holes in the p-n junction, or at grain boundaries. The shunt resistance (R_{sh}) can be obtained using the so-called two points-single curve method from two points on one illuminated I–V curve [19,20]. However, when we consider two operation points on one illuminated I–V curve or two illuminated

* Corresponding author. Tel.: +886 2 3366 5341; fax: +886 2 2362 7620.
E-mail address: jajiang@ntu.edu.tw (J.-A. Jiang).
[1] Equal contribution, co-first authors.

0360-5442/$ – see front matter © 2011 Elsevier Ltd. All rights reserved.
doi:10.1016/j.energy.2011.08.019

I–V curves, it is found that both methods can lead to large errors because of different operating conditions and complicated mathematical operations. Hence, it is difficult to obtain the dynamic resistances of the PV modules (with low calculation burden), simply by using the two-curve method or two points-single curve method [19]. A less complicated way to find the dynamic resistances of the PV modules through a simpler and more convenient estimation technique is required.

Impedance matching is the practice of designing the input impedance of an electrical load or the output impedance of its corresponding signal source in electrical circuits so as to maximize the power transfer and minimize the reflections from the load. In order to gain the maximum power from a PV module at the current solar irradiance level and temperature, it is mandatory to match the PV source with the load by means of switching from a direct current (DC) to direct current converter (DC–to–DC converter). To ensure the source-load matching, the PV generation system should properly change the operating voltage at the terminals of the PV module according to the actual weather conditions. Due to the nonlinear *I–V* characteristic curve of PV modules, it is generally difficult to analyze and determine their output impedance, i.e., dynamic resistance. Hence, it is necessary to develop an efficient method for the determination of the dynamic resistance. Such a method should be able to estimate the voltage value corresponding to the maximum power delivered by the PV source and further achieve impedance matching for any kind of PV module.

The dynamic resistance of solar cells and modules can be determined by an *I–V* characteristic curve. Being a dynamic quantity, the dynamic resistance is normally taken to be the slope or the derivative of the *I–V* characteristic of a cell or a module and is defined as the change in voltage divided by the change in current as $\Delta V_{pv}/\Delta I_{pv}$ or dV_{pv}/dI_{pv}. Furthermore, the dynamic resistance is composed of the series resistance and shunt resistance. However, the effect of the series resistance and shunt resistance is often ignored in the practical quantification of dynamic resistances. Such inaccuracies of the dynamic resistance will lead to the improper PV control operations and to the tracking of incorrect maximum power point (MPP).

As mentioned above, it is still very complicated to obtain the value of the series resistance and shunt resistance which can be done using the two-curve method and the two points-single curve method. This makes it difficult to determine the dynamic resistance using the electrical parameters of a solar cell, i.e., series resistance and shunt resistance. In most cases, electrical circuits are used as interfaces between the PV generators and the loads, or between inverters and the energy accumulators, and operated in off-line mode. A relatively powerful microcontroller is required to implement the above-mentioned methods due to the complexity of the mathematical operations involved.

Focusing on the resistance effect of the solar cells, we propose a new and simple method to directly determine the dynamic resistance of the PV modules from one point on an irradiated current–voltage characteristic curve. This method is developed based on the p-n junction semiconductor theory of solar cells. Through the direct resistance-estimation method, we elucidate the effects of dynamic resistance on the characteristics of PV modules even if the irradiation intensity or ambient temperature is changed. The model of dynamic resistance with a combination of finite series resistance and shunt resistance is also taken into consideration in this study. The correlation between the dynamic resistance and the ambient factors will be discussed in detail in the following sections.

2. Theoretical basis of the proposed method

The p-n junction recombination mechanism of semiconductors successfully describes the nonlinear characteristics of PV modules [17]. The PV modules exhibit extremely nonlinear voltage–ampere characteristics, which vary continually with module temperature and solar illumination. This fact often causes a great deal trouble leading to a lack of control for the proper operation of the PV modules and the tracking of incorrect MPP. To overcome such problems, we propose a novel and simple method to directly determine the dynamic resistance of the PV modules from an irradiated current–voltage characteristic curve. Using the developed method to directly estimate the dynamic resistance of the PV modules, we can control the MPP and achieve the maximum utilization efficiency of the PV modules.

Fig. 1 depicts the equivalent circuit for the PV modules. Using the symbols shown in Fig. 1, the output current I_{pv} of PV modules is given by [17,21,22]

$$I_{pv} = I_{ph} - I_d - V_d/R_{sh}, \tag{1}$$

where I_{ph} is the light-generated photocurrent (A); R_{sh} is the shunt resistance (ohm); and I_d and V_d are the current and voltage of the p-n junction diode, respectively. The current I_d and voltage V_d of the p-n junction diode can be expressed as

$$V_d = V_{pv} + I_{pv}R_s, \tag{2}$$

and

$$I_d = I_{\text{sat}}\left\{\exp\left[\frac{qV_d}{nkT}\right] - 1\right\}, \tag{3}$$

where R_s is the series resistance (ohm); I_{sat} is the reverse saturation current (A); n is the ideality factor of the diode; q is the electron charge (C); k is the Boltzmann's constant (eVK^{-1}); and T is the ambient temperature (K). The ideality factor (n) of the diode is usually set as 1 when only the diffusion current flows across the junction and 2 when the recombination current dominates [17]. Thus, the ideality factor of the diode could be considered constant, and independent of voltage [17]. After substituting the components associated with the p-n junction diode into Eq. (1), the current I_{pv} of PV modules can be expressed by [17,21,22]

$$I_{pv} = I_{ph} - I_{\text{sat}}\left\{\exp\left[\frac{q(V_{pv} + I_{pv}R_s)}{nkT}\right] - 1\right\} - \frac{V_{pv} + I_{pv}R_s}{R_{sh}}. \tag{4}$$

When the load $R_L = 0$ in Fig. 1, the output voltage V_{pv} is zero, and the short-circuit current I_{sc} is given by [23]

$$I_{sc} = I_{ph} - I_{\text{sat}}\left\{\exp\left[\frac{q(I_{sc}R_s)}{nkT}\right] - 1\right\} - \frac{I_{sc}R_s}{R_{sh}}, \tag{5}$$

or

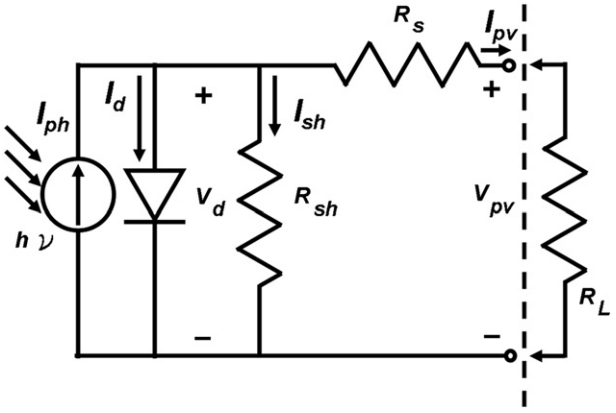

Fig. 1. The equivalent circuit for the PV modules.

$$I_{ph} = I_{sc}\left(1+\frac{R_s}{R_{sh}}\right) - I_{\text{sat}}\left\{\exp\left[\frac{q(I_{sc}R_s)}{nkT}\right]-1\right\}. \quad (6)$$

On the other hand, when the load disconnects, the output current I_{pv} is calculated as

$$0 = I_{ph} - I_{\text{sat}}\left\{\exp\left[\frac{qV_{oc}}{nkT}\right]-1\right\} - \frac{V_{oc}}{R_{sh}}, \quad (7)$$

and the open-circuit voltage V_{oc} is calculated as [24]

$$V_{oc} = \frac{nkT}{q}\ln\left[\frac{I_g + I_{\text{sat}}}{I_{\text{sat}}}\right]. \quad (8)$$

Substituting Eq. (6) into Eq. (7), we can obtain the reverse saturation current I_{sat} as follows:

$$I_{\text{sat}} = \left(I_{sc} - \frac{V_{oc}}{R_{sh}}\right)\exp\left[\frac{-qV_{oc}}{nkT}\right]. \quad (9)$$

In order to directly estimate the dynamic resistance which is defined as the negative reciprocal of dI_{pv}/dV_{pv}, we first differentiate the Eq. (4) with respect to V_{pv}, i.e.,

$$\frac{dI_{pv}}{dV_{pv}} = -\frac{1}{R_{sh}} - \frac{dI_{pv}}{dV_{pv}}\cdot\frac{R_s}{R_{sh}} - I_{\text{sat}}\frac{q}{nkT}\left(1+\frac{dI_{pv}}{dV_{pv}}\cdot R_s\right) \times \exp\left[\frac{q(V_{pv}+I_{pv}R_s)}{nkT}\right], \quad (10)$$

where q and k are constants; n is the ideality factor of the diode; and T is the temperature. For the open-circuit condition and the short-condition of PV modules, two expressions using the slope of one I–V characteristic curve at (V_{oc}, 0) and (0, I_{sc}) points are given by [18]

$$R_{s0} = -\left(\left.\frac{dI_{pv}}{dV_{pv}}\right|_{V_{pv}=V_{oc}}\right)^{-1} \quad (11)$$

and

$$R_{sh0} = -\left(\left.\frac{dI_{pv}}{dV_{pv}}\right|_{I_{pv}=I_{sc}}\right)^{-1}, \quad (12)$$

respectively. When the load is disconnected from the PV modules and the output current I_{pv} is zero, Eq. (10) can be expressed by

$$\left.\frac{dI_{pv}}{dV_{pv}}\right|_{V_{pv}=V_{oc}} = -\frac{1}{R_{sh}} - \left.\frac{dI_{pv}}{dV_{pv}}\right|_{V_{pv}=V_{oc}}\cdot \frac{R_s}{R_{sh}} - I_{\text{sat}}\frac{q}{nkT}\left(1+\left.\frac{dI_{pv}}{dV_{pv}}\right|_{V_{pv}=V_{oc}}\cdot R_s\right) \times \exp\left[\frac{qV_{oc}}{nkT}\right]. \quad (13)$$

Eq. (13) can be further simplified to

$$-\frac{1}{I_{\text{sat}}}\frac{nkT}{q}\left.\frac{dI_{pv}}{dV_{pv}}\right|_{V_{pv}=V_{oc}}\exp\left[\frac{-qV_{oc}}{nkT}\right] \cong 1 + \left.\frac{dI_{pv}}{dV_{pv}}\right|_{V_{pv}=V_{oc}\cdot R_s}. \quad (14)$$

Therefore, the series resistance R_s can be expressed by

$$R_s = -\left(\left.\frac{dI_{pv}}{dV_{pv}}\right|_{I_{pv}=I_{sc}}\right)^{-1} - \frac{1}{I_{\text{sat}}}\frac{nkT}{q}\exp\left[\frac{-qV_{oc}}{nkT}\right] = R_{s0} - \frac{1}{I_{\text{sat}}}\frac{nkT}{q}\exp\left[\frac{-qV_{oc}}{nkT}\right]. \quad (15)$$

On the other hand, the output voltage V_{pv} is zero for the short-circuit condition of PV modules, Eq. (10) can be

$$\left.\frac{dI_{pv}}{dV_{pv}}\right|_{I_{pv}=I_{sc}} = -\frac{1}{R_{sh}} - \left.\frac{dI_{pv}}{dV_{pv}}\right|_{I_{pv}=I_{sc}}\cdot\frac{R_s}{R_{sh}} - I_{\text{sat}}\frac{q}{nkT} \left(1+\left.\frac{dI_{pv}}{dV_{pv}}\right|_{I_{pv}=I_{sc}}\cdot R_s\right)\exp\left[\frac{qI_{sc}R_s}{nkT}\right]. \quad (16)$$

Eq. (16) can be further simplified to

$$\left.\frac{dI_{pv}}{dV_{pv}}\right|_{I_{pv}=I_{sc}} \cong -\frac{1}{R_{sh}} - \left.\frac{dI_{pv}}{dV_{pv}}\right|_{I_{pv}=I_{sc}}\cdot\frac{R_s}{R_{sh}}. \quad (17)$$

Therefore, the shunt resistance R_{sh} can be expressed by

$$R_{sh} \cong -\left(\left.\frac{dI_{pv}}{dV_{pv}}\right|_{I_{pv}=I_{sc}}\right) = R_{sh0}. \quad (18)$$

The values of V_{oc} and I_{sc} can be obtained from the data sheets of the PV modules, and the values of series resistance R_s and shunt resistance R_{sh} can be extracted from one I–V characteristic curve through Eqs. (15) and (18), respectively. Moreover, the reverse saturation current I_{sat} can also be calculated by Eq. (9). To this end, we can directly estimate the value of dynamic resistance from one I–V characteristic curve via Eq. (10) using the values of V_{oc}, I_{sc}, R_s, and R_{sh}.

From the above development, it can be clearly seen that the proposed method is a new and simple approach with a low calculation burden, which can be used to directly determine the dynamic resistance of the PV modules from one point of the irradiated I–V characteristic curve. The characteristic parameters of the PV modules, i.e., R_s and R_{sh}, are dependent on the semiconductor fabrication processes as well as different weather conditions, and can be calculated by Eqs. (15) and (18). Therefore, with Eq. (10), we can directly evaluate the value of dynamic resistance from one I–V characteristic curve. The values of the voltage and the current at the MPP of the PV modules can be directly evaluated using the direct-prediction method based on the p-n junction recombination mechanism. Furthermore, the value of the dynamic resistance at the MPP of the PV modules can also be estimated, and the MPP of the PV modules can be tracked by using the impedance matching method. The direct resistance-estimation method could be thus applied to the maximum power point tracking (MPPT) algorithm for any kind of PV module. By using the proposed method we expect to be able to achieve in real-time the maximum power output for a solar generation system.

3. Experimental procedures

To evaluate the performance of the proposed direct resistance-estimation method, a variety of experiments including both numerical simulation and field tests with respect to PV modules composed of different cell numbers, various irradiation intensities and temperatures were conducted in this work. In order to efficiently determine the dynamic resistance and achieve the impedance matching for any type or combination of PV modules, we used four PV modules composed of different cell numbers and examined the feasibility of the proposed direct resistance-estimation method. The four PV module combinations were comprised of 36, 48, 60 and 72 cells connected in a series. PV modules made of the p-type, multi-crystalline silicon (mc-Si) wafers with a resistivity of around 0.5–3 Ω cm were used for these experiments. The size of each solar cell was 35 × 50 mm^2.

In this study, we conducted field data tests to examine both the temperature-dependent and irradiation intensity-dependent characteristics of the PV modules. Fig. 2 shows a schematic diagram of the field data tests for the temperature-dependent and

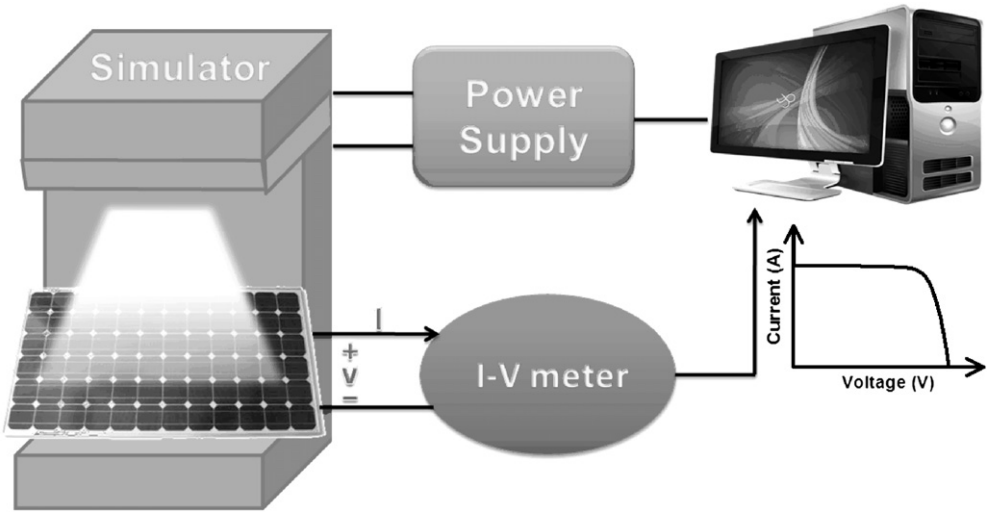

Fig. 2. A schematic diagram of the field data tests for the temperature-dependent and irradiation intensity-dependent characteristics of the PV modules.

irradiation intensity-dependent characteristics of the PV modules. PV modules made up of 60 commercial cells connected in series were used in the field tests. The generated data were used to verify the performance of the proposed direct resistance-estimation method. As a reference, the *I–V* characteristics of the PV modules were first measured with an *I–V* meter under standard test conditions: irradiation intensity of 1000 W/m^2, AM 1.5G, and an ambient temperature at 25 °C. The characteristics of the PV modules under different illumination levels and ambient temperatures were also examined using a solar simulator (SPI-SUN SIMULATOR 4600, Spire). The experiments for these field tests were conducted at three illumination levels of 600, 800, and 1000 W/m^2, and three ambient temperatures of 25, 50, and 75 °C. Under different illumination levels and temperatures, field test data of the *I–V* characteristics were obtained by the *I–V* meter for the same ten PV modules and was repeated 100 times. The numerical simulations were performed with the MATLAB program to 8-digit precision. The MATLAB toolbox, i.e., finite element method, was used to solve the nonlinear differential equations (e.g. Eq. (10) in this paper) and obtain the values of the characteristic parameters for the PV modules [25–27].

4. Results and discussion

We used four PV modules with different cell numbers to examine the feasibility of applying the proposed direct resistance-estimation method to any type or combination of PV modules. Fig. 3 (a) shows the *I–V* (current–voltage) curves of the PV modules with different combinations and different numbers of solar cells under an irradiation intensity of 1000 W/m^2; AM 1.5G; and an ambient temperature of 25 °C. The cell numbers were 36, 48, 60, and 72 and they were connected in a series to form the four respective PV modules. As can be seen in Fig. 3 (a), the open-circuit voltage V_{oc} was gradually augmented while the short-circuit current I_{sc} remained almost constant as the number of PV cells in the modules increased. The proposed method is used to estimate the dynamic resistances of these PV modules with different cell numbers. Through Eqs. (10), (15), and (18), the values of the dynamic resistances are computed based on the values of V_{oc}, I_{sc}, R_s, and R_{sh} acquired from Fig. 3 (a). The solid symbols and dashed lines in Fig. 3 (b) indicate the experimental and calculated dynamic resistances of the PV modules, respectively. As the number of PV cells in the modules increases, the dynamic resistances are imperceptibly raised. The average values of the percentage of prediction error of the actual and estimated dynamic resistance for the PV modules with different cell numbers are 0.56%, 0.13%, −0.25%, and 0.64%, respectively. It is found that both curves look relatively similar,

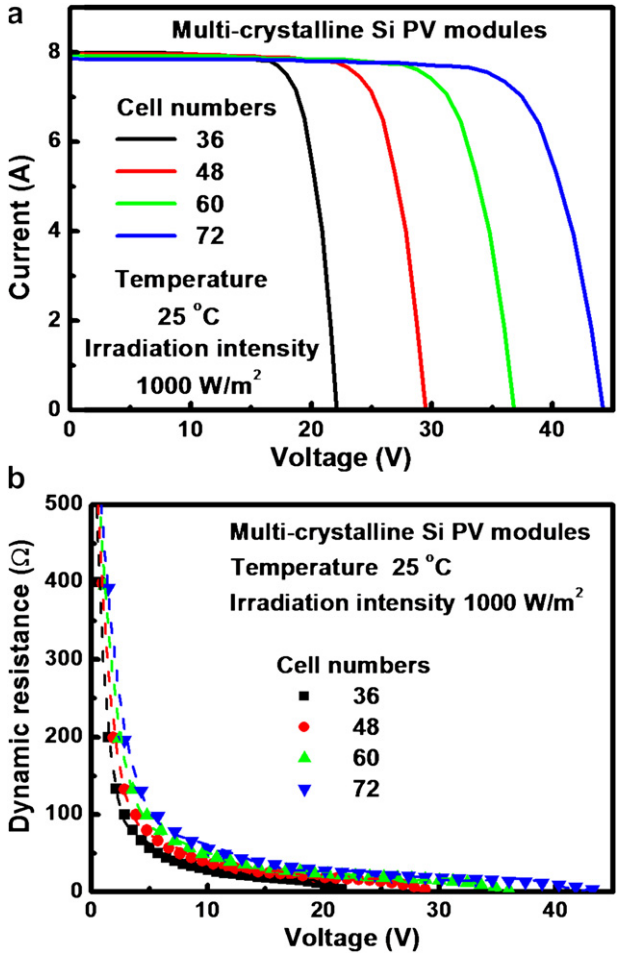

Fig. 3. The characteristic curves of the multi-crystalline Si PV modules: (a) current–voltage characteristic; and (b) dynamic resistance of the PV modules with different cell numbers under an irradiation intensity of 1000 W/m^2; AM 1.5G; and an ambient temperature of 25 °C. The dashed lines in the Fig. 3 (b) indicate the dynamic resistances of the PV modules estimated by the direct resistance-estimation method.

when comparing the calculated dynamic resistances with the experimental values shown in Fig. 3 (b). These experiments show that the proposed method is accurate and simple to use. Our method is an effective way to determine the dynamic resistances of PV modules, from one point of an irradiated current–voltage characteristic curve, by taking the effects of the resistance into consideration. The experimental results demonstrate that the proposed method is feasible for PV modules with different combinations of cell numbers.

The temperature-dependent and irradiation intensity-dependent characteristics of PV modules were both considered in the field data tests. Fig. 4 (a) shows the I–V curve of PV modules with different irradiation intensities and an ambient temperature of 25 °C. Under standard test conditions (irradiation intensity of 1000 W/m^2, AM 1.5G, and an ambient temperature of 25 °C), the open-circuit voltage V_{oc} and the short-circuit current I_{sc} of the PV modules are 36.83 V and 7.86 A, respectively. Moreover, we further investigate the effects of the various irradiation intensities on the I–V curves of the PV modules. Generally, the output power of the PV modules increases with the radiation intensity [17]. Such an increase in the output power is primarily caused by a rise in the open-circuit voltage V_{oc}, and also by the corresponding linear increase in the photocurrent with the irradiation intensity. On the other hand, there is a linear boost in the short-circuit current I_{sc} in line with the minority carrier concentration, due to the increase in irradiation intensity [17]. The I–V curves of the PV modules plotted for different ambient temperatures and an irradiation intensity of 1000 W/m^2 are depicted in Fig. 4 (b). Examination of Fig. 4 (a) and (b) shows that the performance of the PV modules affected by temperature, and that their voltage decreases as the temperature climbs. The decrease in temperature depends on the open-circuit voltage and the band gap of the semiconductor material used to make the PV cell [17]. From Fig. 4 (a) and (b), it can be observed that the changes in irradiation mainly affect the output current, while the changes in temperature mainly influence the output voltage. As the device temperature goes up, I_{sc} slightly increases. However, V_{oc} will rapidly decline due to the exponential dependence of the saturation current I_{sat} on the temperature [17].

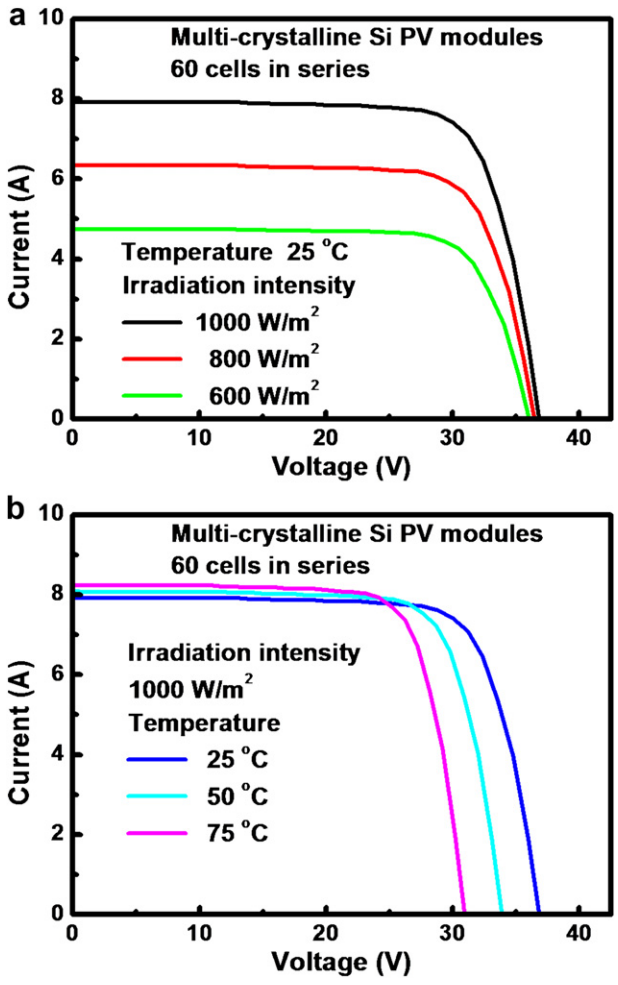

Fig. 4. The current–voltage characteristic of the PV modules: (a) under different irradiation intensities and an ambient temperature of 25 °C; and (b) under different temperatures and an irradiation intensity of 1000 W/m^2.

Next, we conducted field tests under different irradiation intensities while the temperature was maintained at 25 °C. The experimental data were used to plot the dynamic resistances of the PV modules. The hollow symbols and dashed lines in Fig. 5 (a) indicate the experimental and calculated dynamic resistances of the PV modules, respectively. Using Eqs. (10), (15), and (18), the dynamic

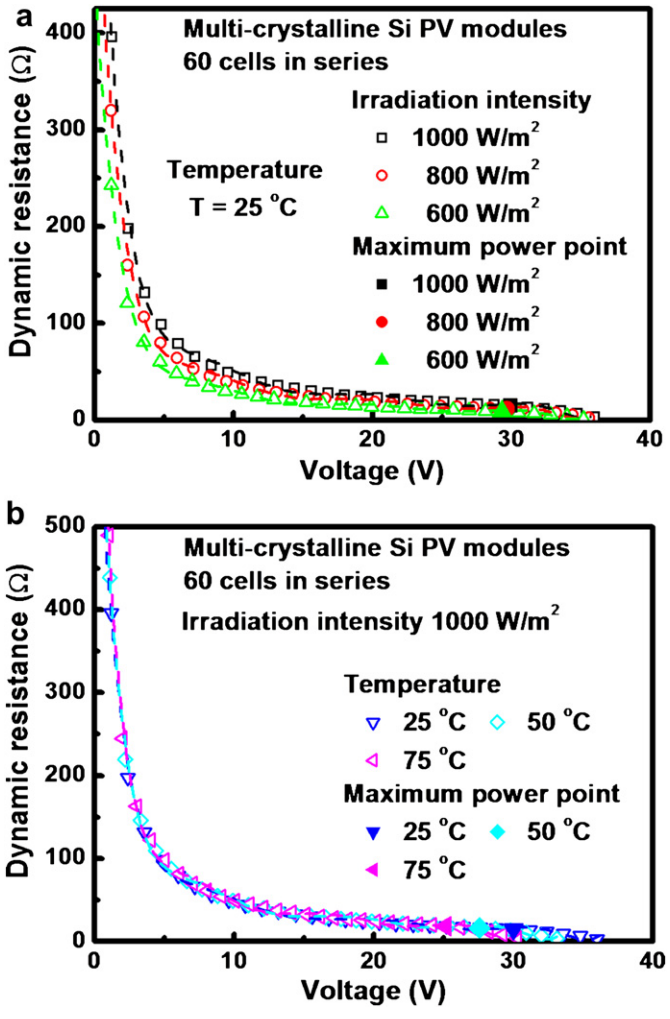

Fig. 5. The dynamic resistance of the PV modules: (a) under different irradiation intensities and an ambient temperature of 25 °C; and (b) under different temperatures and an irradiation intensity of 1000 W/m^2. The dashed lines indicate the dynamic resistances of the PV modules with different irradiation intensities and different temperatures, estimated by the direct resistance-estimation method. The solid symbols indicate the maximum power points of the PV modules: (a) under different irradiation intensities and an ambient temperature of 25 °C; and (b) under different temperatures and an irradiation intensity of 1000 W/m^2, estimated by the direct-prediction method [28].

resistances are calculated by means of the values of V_{oc}, I_{sc}, R_s, and R_{sh}, which are acquired from Fig. 4 (a). The calculated dynamic resistances are also verified through the experimental results shown in Fig. 5 (a). Comparing the calculated dynamic resistances with the experimental ones of PV modules in Fig. 5 (a), it can be seen that both values of dynamic resistances are pretty similar. As the irradiation intensities rise, the average percentage of prediction errors between the actual and estimated dynamic resistances of the PV modules are −0.55%, 0.33%, and −0.90%, respectively. Furthermore, the increase in the dynamic resistance with the irradiation intensity, indicated by the hollow symbols in Fig. 5 (a), is primarily caused by the rise in the open-circuit voltage V_{oc} due to the linear increase of the photocurrent [17]. This is because the short-circuit current increases along with the light-generated carrier concentration as the irradiation intensity increases, resulting in the open-circuit voltage increase [17]. The experimental results verify that the dynamic resistances of the PV modules can also be accurately estimated using the proposed direct resistance-estimation method under various illumination conditions.

The dynamic resistance curves of the PV modules from the experimental data and the ones estimated by Eq. (10) are plotted in Fig. 5 (b). In this test case, temperatures are varied but the irradiation intensity is set at 1000 W/m^2. The hollow symbols and dashed lines in Fig. 5 (b) indicate the experimental and calculated dynamic resistances of the PV modules, respectively. Similarly, the values of V_{oc}, I_{sc}, R_s, and R_{sh} acquired from Fig. 4 (b) are used to compute the dynamic resistances by using Eqs. (10), (15), and (18). Both sets of results are plotted together in Fig. 5 (b) for comparison. In the order of three tested temperatures, the average percentage of prediction errors between the actual and estimated dynamic resistances of the PV modules are −0.90%, 0.24%, and −0.76%, respectively. These average percentage prediction errors are quite small. As the temperature increases, the dynamic resistances increase imperceptibly but remain insensitive to the changes of temperature, because the I_{sc} slightly increases [17]. This experiment shows that the dynamic resistances of the PV modules under various ambient temperatures can be accurately estimated by the proposed direct resistance-estimation method.

To ensure the optimal use of available solar energy and achieve the maximum power output in real time under all of the possible system operation conditions, we need to estimate the dynamic resistances of the PV modules and further ensure source-load matching by properly changing the operating voltage at the terminals of the PV module depending on the actual weather conditions. We can directly obtain the values of the voltage V_{mp} and current I_{mp} at the MPP of the PV modules in real-time by the direct-prediction MPP method [28] even if the irradiation conditions are changed. As shown in Fig. 5 (a) and (b), the solid symbols indicate the MPPs of the PV modules: (a) under different irradiation intensities and an ambient temperature of 25 °C; and (b) under different temperatures and an irradiation intensity of 1000 W/m^2, estimated by the direct-prediction method [28]. The variations in the characteristic parameters and resistances of the PV modules under different illumination levels and temperatures are listed in Tables 1 and 2, respectively. With varying illumination levels and temperatures, the average values of the percentage of prediction error of V_{mp} (%) and I_{mp} (%) between the actual and estimated maximum power points of the PV modules are 0.36% and 0.27%, respectively. These results demonstrate that the voltage V_{mp} and current I_{mp} at the MPP of the PV modules can be simply and accurately estimated using the direct-prediction method.

Furthermore, the value of dynamic resistance at the MPP of the PV modules can also be evaluated by the direct resistance-estimation method. By substituting the values of V_{mp} and I_{mp} at the MPP of the PV modules into Eq. (10) and using the series and shunt resistance of PV modules obtained from the Eqs. (15) and (18), the value of dynamic resistance at the MPP of the PV modules can be directly estimated, even if the irradiation intensities or ambient temperatures are changed. Specifically, the R_s, R_{sh}, and dynamic resistance will all increase with the irradiation intensity and temperature to some extent.

The calculated dynamic resistance and the experimental values at the MPP of the PV modules are listed in Tables 1 and 2 for comparison. We can clearly see that in both cases the results are pretty similar. Using the proposed direct resistance-estimation method, the average percentage of prediction errors of dynamic resistances at the MPP of the PV modules under varying illumination levels and temperatures are 0.986% and 0.886%, respectively. The results indicate that the proposed method can achieve an accurate estimation of the dynamic resistance at the MPP of the PV modules under different temperatures and illumination intensities.

The experiments have shown that the method presented here is a simple, accurate, and has a low calculation burden. It can also determine the values of R_s, R_{sh}, and the dynamic resistance at the MPP of the PV modules from a single irradiated I–V characteristic curve, in which the effects of the resistance are also included. Only the values of V_{oc} and I_{sc} obtained from the data sheet for the PV modules are needed for the direct estimation of accurate values of the dynamic resistances for the PV modules under environmental variations. On the other hand, we have no consideration for the dust accumulation about the PV module under the various operation conditions in this study. For the operation of PV module during the outdoor exposure, it would have dust accumulation on the surface of PV modules and reduce the efficiency of PV module. The fine coating of dust also reflects sunlight off the surface of a PV module preventing maximum light from penetrating through the module glass and into the cells to be converted into energy. We will investigate in depth the relation between the output lowering due to dusted or shaded PV module and the change of I–V characteristics of PV module in future.

Based on the proposed method, the MPP tracking of the PV modules under various weather conditions can be further achieved in practical applications by incorporating our method with the impedance matching method, resulting in obtaining the maximum power output from the PV modules. The effectiveness of the proposed method is verified through experiments. It is expected

Table 1
The dependence of characteristic parameters and resistances for the PV modules on different irradiation intensities under an ambient temperature of 25 °C. The test results were experimentally measured and estimated by the direct-prediction method [28] and direct resistance-estimation method, respectively.

Irradiation intensity (W/m^2)	Experimental results			Direct-prediction method		Direct resistance-estimation method			
	V_{mp} (V)	I_{mp} (A)	dynamic resistance at MPP (Ω)	V_{mp} (V)	I_{mp} (A)	series resistance R_s (Ω)	shunt resistance R_{sh} (kΩ)	dynamic resistance at MPP[a] (Ω)	percentage prediction errors (%)
1000	29.991	7.409	14.82	30.015	7.402	2.21	20.7	14.68	−0.94
800	29.692	5.927	11.97	29.678	5.921	1.78	18.6	12.08	0.92
600	29.334	4.448	9.09	29.312	4.451	1.35	16.4	8.99	−1.10

[a] The values of V_{mp} and I_{mp} at MPP acquired from the direct-prediction method [28] are used to obtain these results.

Table 2
The dependence of characteristic parameters and resistances for the PV modules on different temperatures under irradiation intensity of 1000 W/m^2. The test results were experimentally measured and estimated by the direct-prediction method [28] and direct resistance-estimation method, respectively.

Temperature (°C)	Experimental results			Direct-prediction method		Direct resistance-estimation method			
	V_{mp} (V)	I_{mp} (A)	dynamic resistance at MPP (Ω)	V_{mp} (V)	I_{mp} (A)	series resistance R_s (Ω)	shunt resistance R_{sh} (kΩ)	dynamic resistance at MPP[a] (Ω)	percentage prediction errors (%)
25	29.991	7.409	14.82	30.015	7.402	2.21	20.7	14.68	−0.94
50	27.571	7.571	16.43	27.309	7.608	2.44	22.9	16.56	0.79
75	25.161	7.730	18.35	24.925	7.788	2.72	25.2	18.18	−0.93

[a] The values of V_{mp} and I_{mp} at MPP acquired from the direct-prediction method [28] are used to obtain these results.

that the proposed method can also be applied to the method of MPPT and PV stability in future.

5. Conclusions

In this study, we investigated the effectiveness of the proposed direct resistance-estimation method for PV modules functioning under different irradiation intensities and temperatures. With the p-n junction recombination mechanism and the estimation method, the dynamic resistance and MPP of the PV modules are able to be simply and accurately estimated. The dynamic resistances of the PV modules are compared with the experimentally predicted values. Our method provides more accurate results compared to those of the two points-single curve method, even if the irradiation intensities or ambient temperatures are changed. The effectiveness of the proposed method is verified through experiments under various weather conditions and can also be applied to the method of MPPT and PV stability.

Acknowledgments

This work was financially supported in part by the President of National Taiwan University and the National Science Council of the Executive Yuan, Taiwan, under grant numbers: 98R0529-2, 99R50019-2, NSC 98-2218-E-002-039, NSC 98-2218-E-002-012, NSC 98-3114-E-002-010, and NSC 100-3113-E-002-005. The authors are deeply grateful to Mrs. Debbie Nester for her great help in English editing. We are also grateful to the Editor and the anonymous referees for their invaluable suggestions to improve the paper.

References

[1] Takigawa K, Okada N, Kuwabara N, Kitamura A, Yamamoto F. Development and performance test of smart power conditioner for value-added PV application. Sol Energy Mater Sol Cells 2003;75:547–55.
[2] Sopitpan S, Changmuang P, Panyakeow S. Monitoring and data analysis of a PV system connected to a grid for home applications. Sol Energy Mater Sol Cells 2001;67:481–90.
[3] Close J, Ip J, Lam KH. Water recycling with PV-powered UV-LED disinfection. Renew Energy 2006;31:1657–64.
[4] Park KE, Kang GH, Kim HI, Yu GJ, Kim JT. Analysis of thermal and electrical performance of semi-transparent photovoltaic (PV) module. Energy 2010;35:2681–7.
[5] Sakaki K, Yamada K. CO_2 mitigation by new energy systems. Energy Conv Manag 1997;38:S655–60.
[6] Yamada K, Komiyama H, Kato K, Inaba A. Evaluation of photovoltaic energy systems in terms of economics, energy, and CO_2 emissions. Energy Conv Manag 1995;36:819–22.
[7] Gude VG, Nirmalakhandan N, Deng S. Desalination using solar energy: towards sustainability. Energy 2011;36:78–85.
[8] Kaldellis JK, Kondili E, Filios A. Sizing a hybrid wind-diesel stand-alone system on the basis of minimum long-term electricity production cost. Appl Energy 2006;83:1384–403.
[9] Fragaki A, Markvart T. Stand-alone PV system design: results using a new sizing approach. Renew Energy 2008;33:162–7.
[10] Benghanem M, Mellit A. Radial Basis Function Network-based prediction of global solar radiation data: application for sizing of a stand-alone photovoltaic system at Al-Madinah, Saudi Arabia. Energy 2010;35:3751–62.
[11] Arribas L, Cano L, Cruz I, Mata M, Llobet E. PV–wind hybrid system performance: a new approach and a case study. Renew Energy 2010;35:128–37.
[12] Kaabeche A, Belhamel M, Ibtiouen R. Sizing optimization of grid-independent hybrid photovoltaic/wind power generation system. Energy 2011;36:1214–22.
[13] Dali M, Belhadj J, Roboam X. Hybrid solar–wind system with battery storage operating in grid-connected and standalone mode: control and energy management – experimental investigation. Energy 2010;35:2587–95.
[14] Nema P, Nema RK, Rangnekar S. Minimization of green house gases emission by using hybrid energy system for telephony base station site application. Renew Sust Energ Rev 2010;14:1635–9.
[15] Katti PK, Khedkar MK. Alternative energy facilities based on site matching and generation unit sizing for remote area power supply. Renew Energy 2007;32:1346–62.
[16] Pillai IR, Banerjee R. Renewable energy in India: status and potential. Energy 2009;34:970–80.
[17] Sze SM. Physics of semiconductor devices. 2nd ed. New York: Wiley; 1981.
[18] Bashahu M, Habyarimana A. Review and test of method for determination of the solar cell series resistance. Renew Energy 1995;6:129–38.
[19] Thongpron J, Kirtikara K, Jivacate C. A method for the determination of dynamic resistance of photovoltaic modules under illumination. Sol Energy Mater Sol Cells 2006;90:3078–84.
[20] El-Adawi MK, Al-Nuaim IA. A method to determine the solar cell series resistance from a single *I–V*. Characteristic curve considering its shunt resistance—new approach. Vacuum 2002;64:33–6.
[21] Bose BK, Szczesny PM, Steigerwald RL. Microcomputer control of a residential photovoltaic power conditioning system. IEEE Trans Ind Appl 1985;IA-21:1182–91.
[22] Hua CC, Lin JR, Shen CM. Implementation of a DSP-controlled photovoltaic system with peak power tracking. IEEE Trans Ind Electron 1998;45:99–107.
[23] Mutoh N, Ohno M, Inoue T. A method for MPPT control while searching for parameters corresponding to weather conditions for PV generation systems. IEEE Trans Ind Electron 2006;53:1055–65.
[24] Scarpa V, Buso S, Spiazzi G. Low-complexity MPPT technique exploiting the PV Module MPP locus characterization. IEEE Trans Ind Electron 2009;56:1531–8.
[25] Hrennikoff A. Solution of problems in elasticity by the frame work method. J Appl Mech.-Trans ASME 1941;8:169–75.
[26] Courant R. Variational methods for the solution of problems of equilibrium and vibrations. Bull Amer Math Soc 1943;49:1–23.
[27] Logan DL. A first course in the finite element method. 4th ed. Andover: Thomson Learning; 2006.
[28] Wang JC, Su YL, Shieh JC, Jiang JA. High-accuracy maximum power point estimation for photovoltaic arrays. Sol Energy Mater Sol Cells 2011;95:843–51.